Shams Ghahfarokhi, Payam; Kallaste, Ants; Podgornovs, Andrejs; Belahcen, Anouar; Vaimann, Toomas; Asad, Bilal

# Determination of heat transfer coefficient of finned housing of a TEFC variable speed motor

*Published in:*
Electrical Engineering

*DOI:*
10.1007/s00202-020-01132-1

Published: 10/11/2020

*Document Version*
Peer-reviewed accepted author manuscript, also known as Final accepted manuscript or Post-print

*Please cite the original version:*
Shams Ghahfarokhi, P., Kallaste, A., Podgornovs, A., Belahcen, A., Vaimann, T., & Asad, B. (2020). Determination of heat transfer coefficient of finned housing of a TEFC variable speed motor. *Electrical Engineering*. https://doi.org/10.1007/s00202-020-01132-1

# Determination of Heat Transfer Coefficient of Finned Housing of a TEFC Variable Speed Motor

Payam Shams Ghahfarokhi[1, 2*], Ants Kallaste[2], Andrejs Podgornovs[1], Anouar Belahcen[2, 3], Toomas Vaimann[2], Bilal Asad[2]

[1] Dep. Electrical Machines and Devices, Riga Technical University, Kaļķu iela 1, Riga, Latvia
[2] Dep. Electrical Power Engineering and Mechatronics, Tallinn University of Technology, Ehitajate tee 5, Tallinn, Estonia
[3] Dep. Electrical Engineering and Automation, Aalto University, Espoo, Finland
[*]payam.shams@taltech.ee

**Abstract: This paper proposes the analytical calculation of the heat transfer coefficient from the housing of a totally enclosed fan cooled (TEFC) machine during the active cooling. A particular focus is on the calculation of the heat transfer coefficient from the machine's housing for different fan rotational speeds. The paper describes the challenges and provides solutions to dominate them during the analytical calculation of the heat transfer coefficient a TEFC electrical machine. Finally, the proposed method is validated experimentally on a totally enclosed fan cooled synchronous reluctance motor (SynRM), and good correspondence between the analytical and experimental results is obtained.**

## 1. Introduction

The electrical machine encounters several thermal restrictions. These thermal drawbacks are adjusted by selecting an appropriate cooling method. Different applications of electrical machines require different cooling methods. The proper cooling method of an electrical machine is selected according to several different parameters, e.g., machine application, machine topology, machine current density, speed, the operational environment, cost, and machine size[1], [2].

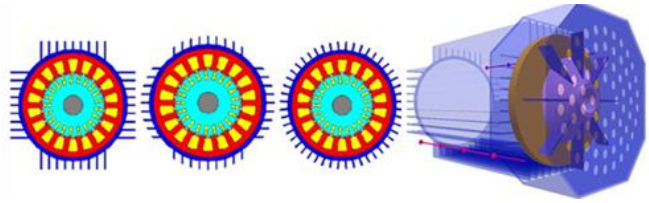

***Fig.1.*** *Different housing structures of TEFC machines* [3],[4] .

The conventional cooling system implemented in industrial electrical motors is a totally enclosed fan cooled (TEFC). In this cooling system, the external fan is attached to the non-driven part of the machine to blow the fluid toward the semi-open fin channels (Fig. 1) [5]. In this approach, the fin channels over the housing are essential[1].

One of the most critical parts of the thermal analysis of TEFC machines is determining the heat transfer from the machine housing to the ambient. The TEFC machine is cooled by passing the coolant over spacing among the semi-open fins of the housing. In comparison to some other active cooling systems, such as the liquid cooling systems, in which the coolant flow rate is predicted with reasonable accuracy, the estimation of the airflow velocity from the housing of a TEFC machine is a challenging task [6]. There are several reasons to describe this statement. The distribution of the airflow produced by the fan is not uniform in every fin channel [6], [7]. According to Fig. 2, by leaking the airflow from semi-open fin channels, the air-speed starts to reduce in the axial orientation [6]. Moreover, some of the fin channels of TEFC housing are blocked by the terminal box and bolt lugs, which terminates in the unbalanced distribution of the airflow about the machine housing [7], [8]. Therefore, calculating the heat transfer coefficient from the housing of TEFC is the conjugate problem, which consists of fluid flow and heat flow problems [6].

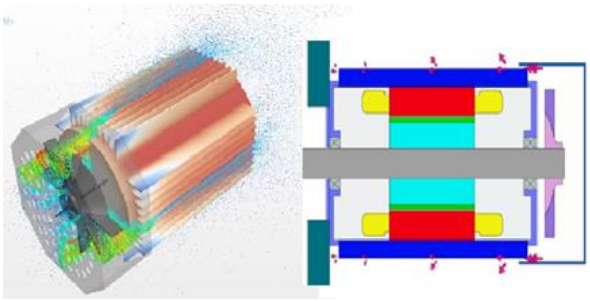

***Fig. 2.*** *Leakage of airflow in the axial orientation* [4].

Different studies consider the thermal analysis of TEFC machines. Mellor in [7] presented one of the earlier studies for these types of machines. In his opinion, the heat transfer coefficient from the housing to the ambient is the only parameter that must be obtained directly from the experiment. In 2003, Boglietti in [9] applied the simplifying assumption to calculate the convection coefficient during the forced cooling. Accordingly, he neglected fins structures of housing and assumed the machine housing as a smooth cylinder and applied the empirical correlation for a horizontal cylinder. In the following, further studies [3], [10], [11] and [12] mainly focused on considering the effect of the airflow behavior in TEFC and just mentioning to calculate the convection coefficient from fin surface using Heilis correlation.

Furthermore, [6] and [13] considered the optimization method for the fin housing structures to find the proper housing structure using the numerical and experimental

methods, respectively. Finally, they found that the airflow distribution and heat transfer from housing directly proportional to the fin housing structure, number of fins, and fin parameters.

However, there is a lack of information about the airflow distribution and airflow speed for 10 kW TEFC machines. Besides, there is no clear view of how to calculate the average heat transfer coefficient of the TEFC machine housing. Consequently, the objective of this study is to enhance knowledge in calculating the heat transfer coefficient from the finned housing of the TEFC machine during the active cooling. The paper focuses on challenges in calculation development. The main objective is to develop the analytical method that can be used to calculate the heat transfer coefficient during active cooling.

For the research purposes, the analytical calculation method described in this study is applied to a four poles 10 kW, 400 V, 50 Hz, TEFC transverse-laminated radial flux SynRM with 'F' insulation class. The analytical method for calculation of heat transfer coefficient is developed and the estimation of its parameters is thoroughly described. To validate the method, a test bench is set up, and measurements are conducted. The experimental results are then compared to these from the proposed method.

## 2. Heat transfer from housing surface

In the active cooling, a significant part of the heat dissipates from a housing surface of TEFC machine to the ambient by the mixture of forced convection and radiation phenomena. The challenging parameter in the calculation of heat transfer from the machine housing to the ambient is the heat transfer coefficient ($h_0$). The heat transfer coefficient ($h_0$) consists of the effect of the radiation and the convection phenomena and is defined as:

$$h_0 = h_c + h_r. \tag{1}$$

where $h_c$ is the convection coefficient (W/m$^2$/K), and $h_r$ is the radiation coefficient (W/m$^2$/K).

Accordingly, in the first step of this section, the calculation of the convection coefficient real frame of a TEFC electrical machine during the active cooling is considered and then extended to determine the radiation coefficient from the actual frame of a TEFC electrical machine.

### *2.1. Forced Convection*

Convection is a heat transfer process between the solid surface and the fluid due to fluid motion[3]. In the active cooling, an external force, for instance, a ventilator, fan, pump, or blower, generates the fluid motion, which is known as the forced convection[3]. The challenging parameter in the calculation of the convection heat transfer is the accuracy of the prediction of the convection coefficient $h_c$.

There are various approaches to determine the forced convection coefficient from the finned housing of a TEFC machine, e.g., computation fluid dynamic (CFD), analytical hydraulic analysis, and empirical correlation [10]. The assessment of the convection coefficient by the CFD and analytical hydraulic analysis is a complex process consisting of sophisticated computing; therefore, the classical empirical correlations are applied to calculate the convection coefficient.

These classical correlations have been developed by the dimensionless numbers, e.g., Prandtl (Pr) and Reynold (Re) numbers [14]. The typical form of the Nusselt number for the forced convection is defined as [3]:

$$\mathrm{Nu} = a(\mathrm{Re})^b(\mathrm{Pr})^c, \tag{2}$$

where $a$, $b$ and $c$ are constants, and Re and Pr are defined as [3]:

$$\mathrm{Re} = \frac{\rho \cdot v \cdot L}{\mu}\ , \tag{3}$$

$$\mathrm{Pr} = \frac{c_p \mu}{k}, \tag{4}$$

where $\rho$ is fluid density (kg/m$^3$), $v$ is fluid rate (m/s), $L$ is the characteristic length of the surface (m), $\mu$ is the fluid dynamic viscosity (kg/s /m), $c_p$ is fluid specific heat capacity (kJ/kg/°C ), and $k$ is fluid thermal conductivity (W/m/°C).

Finally, the correlation between the convection coefficient $h_c$ and the Nusselt number (Nu) is defined as [3], [15]:

$$h_c = \frac{\mathrm{Nu}.k}{L}\ . \tag{5}$$

The empirical correlation for basic flat plate shape and the semi-open fin housing are described hereafter.

1. *Forced convection from a flat plate*

There are various empirical correlations for forced heat transfer over the flat plate. However, According to the flow mode, whether turbulent or laminar, the following well-known correlations for forced convection over the flat plate are applied to calculate the convection coefficient over the smooth surface of the motor [3], [16].

In the laminar mode (Re< 5 ×10$^5$), the Nusselt number is calculated as in [14]:

$$\mathrm{Nu} = 0.664 \cdot \mathrm{Re}^{0.5} \cdot \mathrm{Pr}^{0.33}\ . \tag{6}$$

For the turbulent mode (Re> 5 ×10$^5$), the Nusselt number correlation is defined as [17], [18]:

$$\mathrm{Nu} = (0.037 \cdot \mathrm{Re}^{0.8} - 871) \cdot \mathrm{Pr}^{0.33}. \tag{7}$$

2. *Forced convection coefficient from the semi-open fin housing*

The conventional empirical correlation for calculating the convection coefficient from the finned housing of a TEFC machine during the active cooling was presented by Heiles [3]. This correlation is developed based on different experiments on the actual housing of induction motors, as well as applied some hypotheses; for instance, the airflow is always in a turbulent mode [3], [19] and . The correlation is defined as:

$$h = \frac{\rho\, c_p D_h\, v}{4L}\,(1 - e^{-m})\ , \tag{8}$$

$$m = 0.1448 \frac{L_f^{0.946}}{D_h^{1.16}} \left(\frac{k}{\rho\, c_p v}\right)^{0.214}, \quad (9)$$

where $D_h$ is the hydraulic diameter (m), $v$ is the airflow rate (m/s), and $L_f$ is the axial length of the fin channel (m). According to Heiles's suggestion, the calculated value of the convection coefficient via (8) should multiply to a turbulent factor between 1.7 to 1.9 [3].

### 2.2. Radiation

Radiation is an electromagnetic phenomenon, and the heat is transferred by electromagnetic waves [20], [21]. The amount of heat that can be emitted by this phenomenon entirely depends on the absolute temperature of the body [21].

Radiation is the latest heat transfer phenomenon in the thermal design and analysis of the electrical machine that has attracted the attention of the experts. In addition, it is tough to determine the radiation coefficient experimentally since it is a complex process. Furthermore, in commercial software such as Motor – Cad, they also consider the effect of the radiation on the calculation and thermal modeling of the motor. The radiation occurs in parallel with the convection, and it is difficult to segregate these two phenomena from each other. Accordingly, it is widespread that thermal designers add the convection and the radiation coefficients together as the heat transfer coefficient in their analysis.

The radiation coefficient hr (W/m$^2$/K) is calculated as [21], [22] and [23]:

$$h_r = \varepsilon\sigma F(T_1 + T_2)(T_1^2 + T_2^2). \quad (10)$$

where $\varepsilon$ is the relative emissivity, $\sigma$ is the Stefan-Boltzmann constant equal to $5.67\times10^{-8}$ (W/m$^2$ /K$^4$), $F$ is the view factor; the value of this variable ranges from zero to one, $T_1$ *and* $T_2$ are the temperature of radiating and absorbing surfaces (K) respectively, and indicates the quality of the view between the radiating and absorbing surfaces.

However, the radiation calculation of the fins housing of the electrical machine is more complicated and difficult than that of the smooth electrical machine housings. In particular, the calculation of the view factor is a challenging part of the calculation of the radiation coefficient ($h_r$) [10]. To reduce the complexity of the radiation calculation, a simplifying assumption is used. Accordingly, the whole surface with a clear view of the ambient such as fin base, end caps, and fin tips has a view factor equal to one, and the other with no clear view of the ambient such as fin sides have the view factor equal to zero [4]. According to this assumption, the heat can be transferred to the ambient by radiation phenomenon only from the fin base, fin tips, and end caps. In this thermal network, the same assumption is used to calculate the radiation coefficient from the machine housing.

## 3. Air cooling speed measurement

According to (8), the only unknown parameter with the highest effect on the calculation of the forced convection coefficient is the airflow speed along the semi-open fin channels. To use the empirical correlation, an accurate estimation of the rate of the cooling airflow in each fin channel is necessary. Accordingly, the amount of the speed of the cooling air is measured using a digital hot wire anemometer, and the motor is running under no-load condition. For this purpose, the air velocity meter STI 9545 was used to measure the airflow speed in the circumferential of (semi-open fin channels) the TEFC motor. This tool can measure the rates in the range of 0 to 30 m/s. and the dimension of probe diameter of the tip is 7 mm, which is selected according to the average fin space of TEFC housing. This type of velocity meter has an option called flow set up to choose the appropriate duct shape, e.g., Round duct, rectangular duct, and so on. Furthermore, it has another option as actual and standard set up that the user can also select the standard temperature, standard pressure, and a source for the actual temperature. By using these options, the air velocity meter is calibrated.

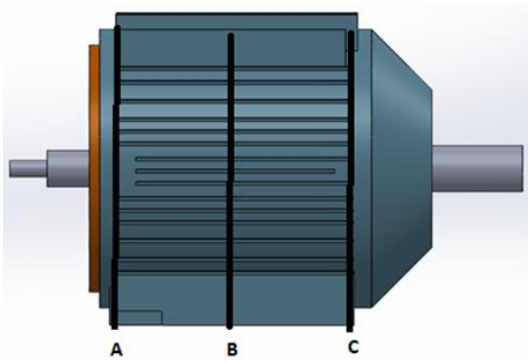


***Fig. 3.*** *Different locations of the air-cooling speed measurement.*

According to Fig. 3, to evaluate the mean speed of an air-cooling flow in the circumference of the machine housing, the airflow speed was measured in three different positions along the axial direction of the cooling fins: at the beginning, in the middle, and at the end of the fins. To increase the measurement accuracy of the mean value of velocity, the velocity samplings are more than 60 points for each fan rotational speed.

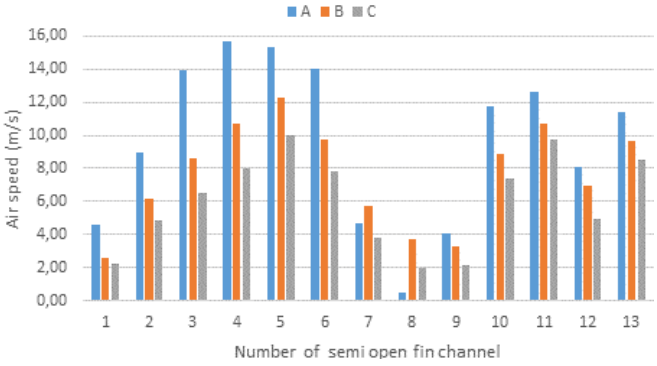


***Fig. 4.*** *Air-speed distributions in the axial direction in several different semi-open fin channels.*

Figure 4 illustrates the air-speed distributions along the axial direction of the several semi-open fin channels for the machine under study. Furthermore, Fig. 4 shows the airflow distribution from top to bottom; for example, Fin 1 is located at the top of the housing, and fin 13 is located at the bottom. Accordingly, it proves that the airflow is not distributed uniformly in the semi-open fin channels; furthermore, predicting the amount of the reduction in the velocity of the airflow is a complex process and depends on

several factors such as fan characteristics, fins dimensions, motor fan cowls. Moreover, as Fig .4 shows, the trend of air in the fins 7 and 8 change. This occurs because the semi-open fin channel s 7 and 8 are located in places that the nameplate of the machine was installed previously; for this test, we removed the nameplate. Accordingly, the width of the fins is smaller than other parts; consequently, as the height of the fins is lower than other parts, in this area, the value of the airflow in the active region is higher than in other parts.

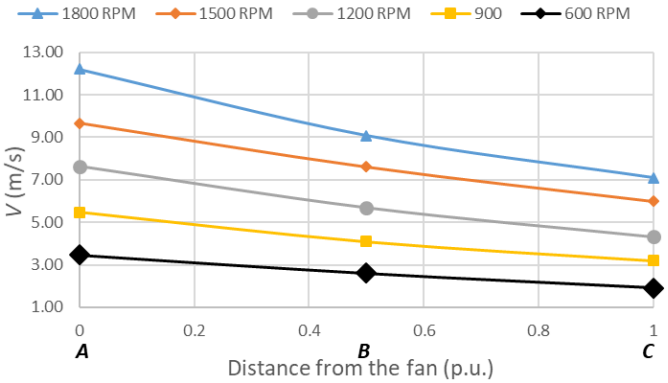


***Fig. 5.*** *Air velocity along the axial direction versus the distance from the fan.*

Figures 5 shows the average airflow speed in each sector for five different fan rotational speeds from 600 rpm to 1800 rpm. As expected, by increasing the distance from the fan, the air-cooling rate starts to decrease due to the leakage. Fig.6 shows the amount of the difference between inlet airflow speed and outlet airflow speed. The average amount of the reduction in the air-cooling rate is around 40% of the inlet velocity. Also, the graph shows the cooling air speed versus the fan rotational speed. The complexity of the cooling air-speed is increased by non- uniform distribution of the air-speed around the housing, especially, the fan cowl supports do not provide a constant distribution of the airflow on the the semi-open fin channels. The prediction of the amount of reduction in airflow speed is a complex function of different factors, including the fan, fin, and cowling design and rotational speed. Furthermore, it shows the effect of the fan velocity for airflow; for instance, the value of the airflow speed at 1800 rpm is 12.25 m/s and drop to 7.09 m/s while at 600-rpm in section A is around 3.46 m/s and in section c drop to 1.92 m/s.

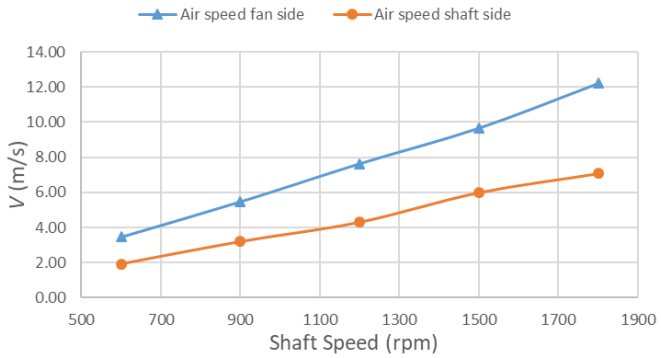


***Fig. 6.*** *Air velocity along the axial direction versus the fan speed in the fan and shaft sides.*

Several different technical papers such as [3], [24], and [25] provide the typical form of the reduction in the velocity versus the distance from the fan for TEFC machines with varying ranges of power, which is operating at 50 Hz. Accordingly, Fig. 7 provides the velocity reduction verses the distance from the fan for 4-pole 10 kW TEFC machine with red dashed lines along with other machine graphs which were presented [3], [24], and [25]. Fig. 7 provides the starting value for the airflow in along the fin channels during the thermal analysis of TEFC machine.

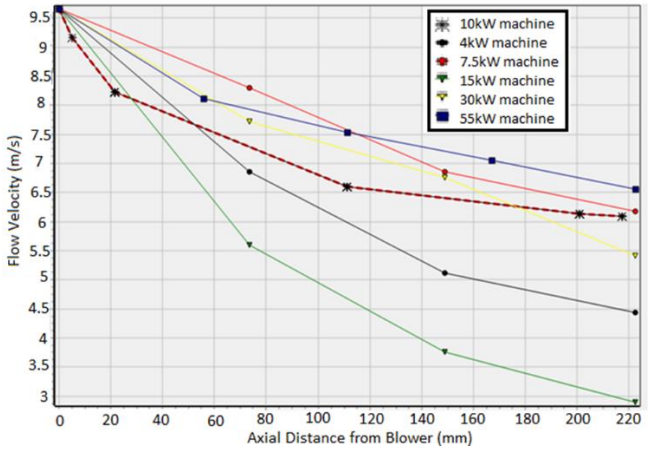


***Fig. 7.*** *The typical form of airflow reduction in semi-open fin channels with distance from the fan* [3], [24], and [25] .

## 4. Analytical analysis method

Figure 8 (a) illustrates the real frame of the machine, which consists of semi-open fin channels and a terminal box. However, in the analytical calculation is assumed that the machine surface is covered entirely by semi-open fin channels. Therefore, the terminal box is neglected in the analytical calculation (Fig. 8 (b)), and the effect of the terminal box applies as the blockage factor in the calculation process.

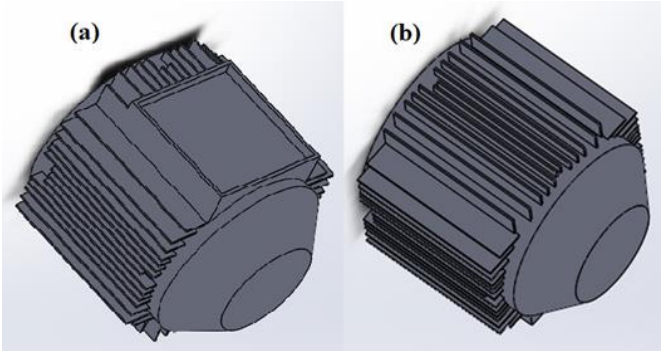


***Fig. 8.*** *The portrayal of the considered setup: (a) real housing, (b) Simplified housing.*

For this case study, the machine is installed in the horizontal direction. As the axial length of the fins, spaces between the fins, and the height of the fins are different; the mean value of the fins parameters of the housing is calculated. Accordingly, Table 1 shows the characteristic data of the fin section of the machine housing at a diameter of 230 (mm).

**Table 1** Characteristic data of the fin section

| | Mean fin's length (mm) | Mean fin's height (mm) | Mean fin's spacing (mm) | Number of fins |
|---|---|---|---|---|
| Semi-open fin channel | 181.51 | 24.29 | 10.6 | 54 |

To calculate the forced convection coefficient from the housing surface of the TEFC electrical machine using the empirical correlations and applying the leakage effect on the air-cooling speed during the computation process, the housing of the machine is divided into three main sections: rear section near the fan, active part, and front section. Then, the amount of the forced convection coefficient is calculated based on the appropriate empirical correlation. Furthermore, the amount of radiation is calculated by using the same method discussed in the previous chapter.

Table 2 shows the segmentation of the machine housing and related empirical correlation for calculating the value of the forced convection coefficient and the radiation phenomenon.

**Table 2** Segmentation of the TEFC housing for the forced convection coefficient

| Component | Empirical Correlation | Air velocity (p.u) | Emissivity | View Factor | Area ($m^2$) |
|---|---|---|---|---|---|
| **End cap (rear)** | Flat plate | 1 | 0.8 | 1 | 0.0415 |
| **Fins base (rear)** | Fin channel | 1 | 0.8 | 1 | 0.0128 |
| **Fin side (rear)** | Fin channel | 1 | 0.8 | 0 | 0.0585 |
| **Fin tips (rear)** | Flat plate | 1 | 0.8 | 1 | 0.0031 |
| **Fins base (active)** | Fin channel | 0.8 | 0.8 | 1 | 0.0908 |
| **Fin side (active)** | Fin channel | 0.8 | 0.8 | 0 | 0.4150 |
| **Fin tips (active)** | Flat plate | 0.8 | 0.8 | 1 | 0.0219 |
| **Fins base (front)** | Fin channel | 0.6 | 0.8 | 1 | 0.0128 |
| **Fin side (front)** | Fin channel | 0.6 | 0.8 | 0 | 0.0128 |
| **Fin tips (front)** | Flat plate | 0.6 | 0.8 | 1 | 0.0031 |
| **End cap (front)** | Flat plate | 0.5 | 0.8 | 1 | 0.0415 |

To apply the effect of fin blockage in the calculation of the forced convection coefficient, the blockage factor ($K_{bl}$) is defined based on the total number of fins ($N_{total}$) and the number of block fins ($N_{block}$) as in [25]:

$$K_{bl} = \frac{N_{total} - N_{block}}{N_{total}}, \tag{11}$$

In the following, the blockage factor is multiplied to the calculated value of the convection coefficient of semi-open fin channels by Heiles correlation. In this study, 12 fins are blocked by the terminal box. By using (11), the blockage factor equals 0.778.

After the calculation of the convection and the radiation coefficient of each segregated shape of the machine housing, the total heat transfer coefficient ($h_0$) is calculated using:

$$h_0 = \sum \frac{h_i A_i}{A_T}, \tag{12}$$

where $h_i$ is the heat transfer coefficient from shape $i$ (W/ $m^2$/K), $A_i$ is the area occupied by shape $i$ ($m^2$), and $A_T$ is the total housing surface of the machine housing ($m^2$).

## 5. Experimental methodology and analysis

The objective of the test setup is to investigate the heat transfer coefficient from the housing of the TEFC electrical machine during air force cooling with different fan speeds. Another objective is to find and verify the accuracy of the analytical calculation by comparing the analytical data to the experimental data. Besides, it considers the effect of the convection coefficient on the amount of temperature of the winding and surface one.

### *5.1. Experimental methodology*

Figure 9 shows the diagram of the test setup. Accordingly, to rotate the cooling fan, the shaft of SynRM was coupled to the shaft of an induction motor. For producing different fan rotational speeds, the speed of the induction motor is adjusted by a frequency converter.

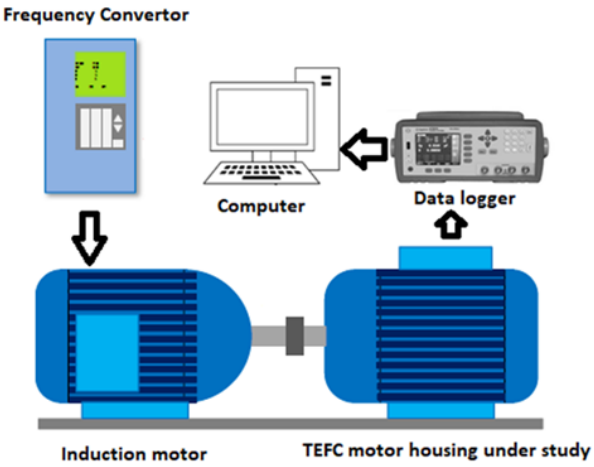


***Fig. 9.*** *The diagram of the experimental setup.*

To better identify the convection phenomenon, it is essential to define the system only based on the stator joule losses; accordingly, as shown in Fig. 10, the rotor of the SynRM machine was replaced by a shaft. Then the cooling fan was assembled at the end part of the shaft.

***Fig. 10.*** *Replacement of the rotor of SynRM with the shaft.*

Figure 11 shows the test setup. Accordingly, the DC stator experiment is a standard test method to determine the convection coefficient. For this purpose, the three-phase stator windings of the SynRM are connected in series and are supplied through a DC power supply. During the experiments, in addition to the injected power to the stator windings, the temperature of the machine housing, end winding, slots, and inlet flow are measured at different locations. The motor has equipped with six thermal sensors (PT-100). The three sensors (PT-100) have been located inside slots, and the rest of them installed at the end winding of each phase of stator windings to monitor the slot temperature and end windings temperatures, respectively.

Furthermore, four k-type sensors have been attached by adhesive materials to the machine housing, and one k-type has connected to the cowl of the machine to monitor the surface temperatures and inlet air temperature, respectively. During the experiments, all the temperature data are collected using a Key sight logger. The test is carried out for each air-cooling speed until the system reached its steady-state condition. According to the standard, the object reaches its steady-state mode when the difference between the measured temperatures during the half an hour less than 0.5 Kelvin. Accordingly, the housing reached its steady-state mode bout 75 min. The experimental procedure is repeated for five different fan rotational speeds: 600, 900, 1200, 1500, and 1800 rpm.

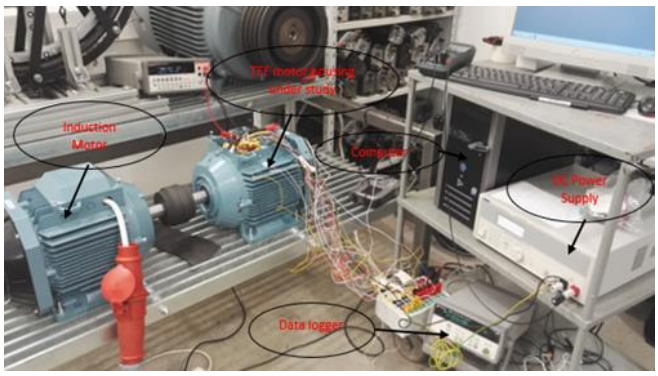


***Fig. 11.*** *Experiment setup.*

### *5.2. The analysis method of experimental data*

The total heat ($Q_T$) generated in the stator winding equals to the total injected electrical power and is defined as:

$$Q_T = V \cdot I, \tag{13}$$

where $V$ equals the input voltage (V), and $I$ is the input current (A).

Since the total heat is extracted to ambient by a mixture of the convection and radiation phenomena; therefore, the total heat is segregated as:

$$Q_T = Q_{conv} + Q_{rad}, \tag{14}$$

where $Q_{conv}$ (W) and $Q_{rad}$ (W) are the amount of heat transferred by convection, and radiation, respectively.

Finally, the heat transfer coefficient $h_0$ is calculated as [22], [23]:

$$h_0 = \frac{Q_T}{(T_s - T_a)A_T}, \tag{15}$$

where $T_s$ is the mean surface temperature (°C), $T_a$ is the inlet airflow temperature (°C).

## 6. Results and Discussions

To effectively validate and evaluate the performance of the analytical method and to gain details about the accuracy of the method in the prediction of heat transfer coefficient form the machine housing during the active cooling, an experimental verification stage is carried out, and the experimental results are compared with the analytical ones.

In the experimental part, to determine the heat transfer coefficient from the experimental data; first, the total heat $Q_T$ is calculated by (13), then according to the inlet airflow temperature and mean surface temperatures of the case study, the heat transfer coefficient $h_0$ is determined by (15).

For the analytical objective, the machine frame is divided into two main sections: endcaps and semi-open fin channels housing, the convection coefficient for the end caps are calculated by (6) or (7) according to the airflow speed. For the semi-open fin channels, this surface is segregated into three different sections, rear, active, and front parts, and according to the hypothesis, the entire surface is covered by semi-open fin channels. According to the airflow speed, the convection coefficient of each section is calculated by (8). Then the effect of the terminal box is added as the blockage factor. Furthermore, the radiation coefficient of each shape is calculated by using the simplification assumption. According to this assumption, the heat can be transferred to the ambient by radiation phenomenon only from the fin base, fin tips, and end caps. After the calculation of the convection and the radiation coefficient of each segregated shape of the machine housing, the total heat transfer coefficient ($h_0$) is calculated by (12).

For the ease of comparing the experimental and analytical results, the data are plotted against the fan rotational speed. It should be noted that the maximum uncertainty in the computed heat transfer coefficients and measured speed are respectively 6.2% and 3%. The calculation procedure of uncertainty was presented in [26]. Moreover, the uncertainty values are displayed as error bars in Fig. 12.

Table 3 shows the analytical data of the heat transfer coefficient from the housing of the TEFC electrical machine.

**Table 3** Analytical data for the air forced cooling

| Shaft speed (rpm) | Inlet speed (Position A) (m/s) | $T_s$ (°C) | $T_a$ (°C) | $h_0$ (W/m$^2$/K) |
|---|---|---|---|---|
| **600** | 3.5 | 32.3 | 22.3 | 20.3 |
| **900** | 5.5 | 29 | 21.2 | 27.9 |
| **1200** | 7.6 | 29.1 | 22.3 | 35.4 |
| **1500** | 9.7 | 28.4 | 22.2 | 41.9 |
| **1800** | 12.2 | 27.3 | 21.8 | 49.8 |

Table 4 shows the experimental data of the heat transfer coefficient from the housing of the TEFC electrical machine. The heat transfer coefficient was calculated by using (12).

**Table 4** Experimental data for the air forced cooling

| Shaft speed (rpm) | Inlet speed (Position A) (m/s) | $T_s$ (°C) | $T_a$ (°C) | $Q_T$ (W) | $h_0$ (W/m²/K) |
|---|---|---|---|---|---|
| **600** | 3.5 | 32.3 | 22.3 | 189.3 | 26.6 |
| **900** | 5.5 | 29 | 21.2 | 190.6 | 34.3 |
| **1200** | 7.6 | 29.1 | 22.3 | 190.7 | 39.3 |
| **1500** | 9.7 | 28.4 | 22.2 | 192 | 43.5 |
| **1800** | 12.2 | 27.3 | 21.8 | 192.2 | 49 |

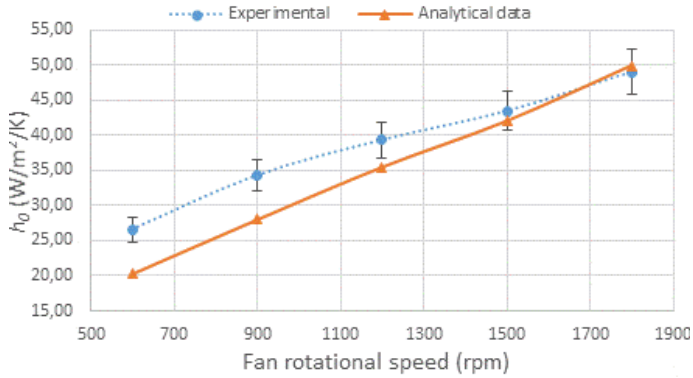


***Fig. 12.*** *Variation of the heat transfer coefficient via the fan's rotational speed.*

Figure 12 shows the variation of the total heat transfer coefficient ($h_0$) versus the fan rotational speed. According to the variety of the experimental value of $h_0$ versus the fan rotational speed, it clearly shows the point when the flow is in turbulent mode. At 1500 rpm and after this point, a rapid increase occurred in the amount of the heat transfer coefficient. In addition, according to the analytical data, by increasing the speed, the amount of the relative difference between the analytical and experimental data starts to decrease, and when the flow is in the turbulent mode, the analytical data merge to the experimental one. The amount of the relative mean difference between the experimental and analytical data is about 11%. In addition, the maximum difference between the experimental and analytical data is 24%, and the minimum is around 3%. Furthermore, by increasing the fan rotational speed, the mean difference between analytical and experimental data is decreased. The maximum mean difference happens in low rotational speed (600 rpm), and it can be concluded that the airflow is not in the turbulent mode.

Figure 13 illustrates the temperature rise in the three different sections of the electrical machines slot, end winding, and machine housing during the experiments. Accordingly, by increasing the fan rotational speeds, the temperature rise also starts to decrease. Furthermore, the heat transfer coefficients increased, and the machine becomes cooler.

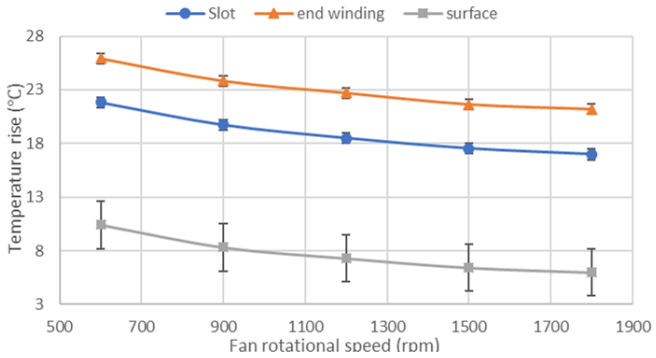


***Fig. 13.*** *The average temperature rise of slots, end windings, and housing for varying fan rotational speed.*

## 7. Conclusion

Most of the power losses in the electrical machine are extracted in the form of the heat to the ambient from the finned housing of TEFC machines. Therefore, calculation of the heat transfer coefficient from the housing of TEFC motor is one of the critical parameters in the thermal modeling and thermal analysis of these types of motors, which has a significant impact on the accuracy of the thermal model.

This paper proposed the analytical method to calculate the heat transfer coefficient from the housing of TEFC machines during the active cooling method. A particular focus was on the calculation of the heat transfer coefficient from the machine's housing for different fan rotational speeds. Furthermore, it provided several solutions to dominate the challenges, e.g., air leakage, blockage. In addition, it proposed the simplifying method to calculate the radiation coefficient from the complex finned structure of the housing.

Finally, the analytical calculation method was validated by experiments. The experimental results demonstrated that the proposed analytical method could be used to calculate the heat transfer coefficient of the housing surface of TEFC machine.

## 8. Acknowledgments

This work has been supported by the European Regional Development Fund within the Activity 1.1.1.2 "Post-doctoral Research Aid" of the Specific Aid Objective 1.1.1 "To increase the research and innovative capacity of scientific institutions of Latvia and the ability to attract external financing, investing in human resources and infrastructure" of the Operational Programme "Growth and Employment" (No.1.1.1.2/VIAA/3/19/501).

## 9. References

[1] M. Rosu *et al.*, *Multiphysics simulation by design for electrical machines, power electronics and drives*, 1st ed. Wiley-IEEE Press, 2017.

[2] Y. C. Chong, "Thermal Analysis and Air Flow Modelling of Electrical Machines," The University of Edinburgh, 2015.

[3] D. A. Staton and A. Cavagnino, "Convection Heat Transfer and Flow Calculations Suitable for Electric Machines Thermal Models," *IEEE Trans. Ind. Electron.*, vol. 55, no. 10, pp. 3509–3516, Oct. 2008.

[4] "Motor-CAD Software by Motor Design - EMag, Therm and Lab." [Online]. Available: https://www.motor-design.com/motor-cad-software/.

[5] S. Mizuno, S. Noda, M. Matsushita, T. Koyama, and S. Shiraishi, "Development of a totally enclosed fan-cooled traction motor," *IEEE Trans. Ind. Appl.*, vol. 49, no. 4, pp. 1508–1514, 2013.

[6] S. Ulbrich, J. Kopte, and J. Proske, "Cooling fin optimization on a TEFC electrical machine housing using a 2-D conjugate heat transfer model," *IEEE Trans. Ind. Electron.*, vol. 65, no. 2, pp. 1711–1718, 2018.

[7] P. H. Mellor, D. Roberts, and D. R. Turner, "Lumped parameter thermal model for electrical machines of TEFC design," *IEE Proc. B Electr. Power Appl.*, vol. 138, no. 5, p. 205, 1991.

[8] K. Ronnberg and M. E. Beniakar, "Thermal Modelling of Totally Enclosed Fan Cooled motors," in *Proceedings - 2018 23rd International Conference on Electrical Machines, ICEM 2018*, 2018, pp. 2619–2625.

[9] A. Boglietti, A. Cavagnino, M. Lazzari, and M. Pastorelli, "A simplified thermal model for variable-speed self-cooled industrial induction motor," *IEEE Trans. Ind. Appl.*, vol. 39, no. 4, pp. 945–952, Jul. 2003.

[10] A. Boglietti, A. Cavagnino, and D. Staton, "Determination of critical parameters in electrical machine thermal models," *IEEE Trans. Ind. Appl.*, vol. 44, no. 4, pp. 1150–1159, 2008.

[11] M. A. Valenzuela, J. A. Tapia, and J. A. Rooks, "Thermal evaluation of TEFC induction motors operating on frequency-controlled variable-speed drives," *IEEE Trans. Ind. Appl.*, vol. 40, no. 2, pp. 692–698, Mar. 2004.

[12] A. Boglietti, A. Cavagnino, and D. A. Staton, "TEFC induction motors thermal models: A parameter sensitivity analysis," *IEEE Trans. Ind. Appl.*, vol. 41, no. 3, pp. 756–763, May 2005.

[13] M. A. Valenzuela and J. A. Tapia, "Heat transfer and thermal design of finned frames for TEFC variable-speed motors," *IEEE Trans. Ind. Electron.*, vol. 55, no. 10, pp. 3500–3508, 2008.

[14] Y. Gai *et al.*, "Cooling of automotive traction motors: Schemes, examples, and computation methods," *IEEE Trans. Ind. Electron.*, vol. 66, no. 3, pp. 1681–1692, Mar. 2019.

[15] D. G. Nair, T. Jokinen, and A. Arkkio, "Coupled analytical and 3D numerical thermal analysis of a TEFC induction motor," in *2015 18th International Conference on Electrical Machines and Systems, ICEMS 2015*, 2016, pp. 103–108.

[16] P. Shams Ghahfarokhi, A. Kallaste, T. Vaimann, A. Rassolkin, and A. Belahcen, "Determination of forced convection coefficient over a flat side of coil," in *2017 IEEE 58th International Scientific Conference on Power and Electrical Engineering of Riga Technical University (RTUCON)*, 2017, pp. 1–4.

[17] F. P. Incropera, D. P. DeWitt, T. L. Bergman, and A. S. Lavine, *Fundamentals of Heat and Mass Transfer*. 2007.

[18] P. Shams Ghahfarokhi, A. Kallaste, A. Belahcen, and T. Vaimann, "Determination of Heat Transfer Coefficient for the Air Forced Cooling Over a Flat Side of Coil," *Electr. Control Commun. Eng.*, vol. 15, no. 1, pp. 15–20, Sep. 2019.

[19] F. Ahmed and N. C. Kar, "Analysis of End-Winding Thermal Effects in a Totally Enclosed Fan-Cooled Induction Motor with a Die Cast Copper Rotor," *IEEE Trans. Ind. Appl.*, vol. 53, no. 3, pp. 3098–3109, May 2017.

[20] J. Pyrhönen, T. Jokinen, and V. Hrabovcová, *Design of Rotating Electrical Machines*. Wiley, 2008.

[21] M. Popescu, D. A. Staton, A. Boglietti, A. Cavagnino, D. Hawkins, and J. Goss, "Modern Heat Extraction Systems for Power Traction Machines - A Review," *IEEE Trans. Ind. Appl.*, vol. 52, no. 3, pp. 2167–2175, May 2016.

[22] M. Markovic, L. Saunders, and Y. Perriard, "Determination of the Thermal Convection Coefficient for a Small Electric Motor," in *Conference Record of the 2006 IEEE Industry Applications Conference Forty-First IAS Annual Meeting*, 2006, vol. 1, pp. 58–61.

[23] O. Meksi and A. O. Vargas, "Numerical and experimental determination of external heat transfer coefficient in small TENV electric machines," in *2015 IEEE Energy Conversion Congress and Exposition (ECCE)*, 2015, pp. 2742–2749.

[24] A. Boglietti and A. Cavagnino, "Analysis of the endwinding cooling effects in TEFC induction motors," *IEEE Trans. Ind. Appl.*, vol. 43, no. 5, pp. 1214–1222, 2007.

[25] D. Staton, A. Boglietti, and A. Cavagnino, "Solving the More Difficult Aspects of Electric Motor Thermal Analysis in Small and Medium Size Industrial Induction Motors," *IEEE Trans. Energy Convers.*, vol. 20, no. 3, pp. 620–628, Sep. 2005.

[26] P. Shams Ghahfarokhi, A. Kallaste, T. Vaimann, A. Rassolkin, and A. Belahcen, "Determination of natural convection heat transfer coefficient over the fin side of a coil system," *Int. J. Heat Mass Transf.*, vol. 126, pp. 677–682, Nov. 2018.